11-1-2021

Identifying the neurophysiological effects of memory-enhancing amygdala stimulation using interpretable machine learning

Mohammad S E Sendi
Emory University

Cory S Inman
University of Utah

Kelly R Bijanki
Baylor College of Medicine

Lou Blanpain
Emory University

James K Park
Emory University

See next page for additional authors

Brain Stimulation 14 (2021) 1511–1519

Contents lists available at ScienceDirect

Brain Stimulation

journal homepage: http://www.journals.elsevier.com/brain-stimulation

Identifying the neurophysiological effects of memory-enhancing amygdala stimulation using interpretable machine learning

Mohammad S.E. Sendi [a, b], Cory S. Inman [c], Kelly R. Bijanki [d], Lou Blanpain [e], James K. Park [g], Stephan Hamann [f], Robert E. Gross [a, g, h], Jon T. Willie [i], Babak Mahmoudi [a, j, *]

[a] Wallace H. Coulter Department of Biomedical Engineering at Georgia Institute of Technology and Emory University, 313 Ferst Dr NW, Atlanta, 30332, GA, USA
[b] Department of Electrical and Computer Engineering at Georgia Institute of Technology, 777 Atlantic Dr, Atlanta, GA, 30313, USA
[c] Department of Psychology at University of Utah, 380 1530 E, Salt Lake City, UT, 84112, United States
[d] Department of Neurosurgery at Baylor College of Medicine, 7200 Cambridge St 9th Floor, Houston, TX, 77030, USA
[e] Neuroscience Graduate Program at Emory University, 1462 Clifton Rd. Suite 314, Atlanta, GA, 30322, USA
[f] Department of Psychology at Emory University, 36 Eagle Row, Atlanta, GA, 3032, USA
[g] Department of Neurosurgery at Emory University, 100 Woodruff Circle, Atlanta, GA, 30322, USA
[h] Department of Neurology at Emory University, 12 Executive Park Dr NE, Atlanta, GA, 30322, USA
[i] Department of Neurology at Washington University School of Medicine in Saint Louis, 660 S. Euclid Avenue Campus Box 8057 St, Louis, MO, 63110, USA
[j] Department of Biomedical Informatics at Emory University, 100 Woodruff Circle, Atlanta, GA, 30322, USA

ARTICLE INFO

Article history:
Received 5 December 2020
Received in revised form
13 September 2021
Accepted 17 September 2021
Available online 5 October 2021

Keywords:
Interpretable machine learning
Amygdala stimulation
Memory
Neurophysiological biomarkers
Feature learning
Hippocampus
Local field potential

ABSTRACT

Background: Direct electrical stimulation of the amygdala can enhance declarative memory for specific events. An unanswered question is what underlying neurophysiological changes are induced by amygdala stimulation.
Objective: To leverage interpretable machine learning to identify the neurophysiological processes underlying amygdala-mediated memory, and to develop more efficient neuromodulation technologies.
Method: Patients with treatment-resistant epilepsy and depth electrodes placed in the hippocampus and amygdala performed a recognition memory task for neutral images of objects. During the encoding phase, 160 images were shown to patients. Half of the images were followed by brief low-amplitude amygdala stimulation. For local field potentials (LFPs) recorded from key medial temporal lobe structures, feature vectors were calculated by taking the average spectral power in canonical frequency bands, before and after stimulation, to train a logistic regression classification model with elastic net regularization to differentiate brain states.
Results: Classifying the neural states at the time of encoding based on images subsequently remembered versus not-remembered showed that theta and slow-gamma power in the hippocampus were the most important features predicting subsequent memory performance. Classifying the post-image neural states at the time of encoding based on stimulated versus unstimulated trials showed that amygdala stimulation led to increased gamma power in the hippocampus.
Conclusion: Amygdala stimulation induced pro-memory states in the hippocampus to enhance subsequent memory performance. Interpretable machine learning provides an effective tool for investigating the neurophysiological effects of brain stimulation.

1. Introduction

Quantifying the neurophysiological effects of brain stimulation is crucial for understanding the underlying mechanisms by which stimulation affects cognitive processes. Such an understanding can pave the way for developing more effective neuromodulation

* Corresponding author. Department of Biomedical Informatics at Emory University, 100 Woodruff Circle, Atlanta, GA, 30322, USA
E-mail address: b.mahmoudi@emory.edu (B. Mahmoudi).

https://doi.org/10.1016/j.brs.2021.09.009

strategies. Moments of relative emotional arousal tend to be remembered better than moments without such arousal, and the amygdala is a key node in the distributed emotion and memory circuits underlying this prioritization of memory [1]. Studies in rodents support the view that the amygdala, particularly the basolateral complex of the amygdala (BLA), is activated by arousal and that it can modulate memory processes in downstream regions such as the hippocampus [2]. However, the mechanisms through which these BLA inputs act remain unknown. One possibility is that direct activation of the BLA could enhance memory without necessitating emotional arousal. Indeed, previous studies in rats have shown that direct electrical stimulation of the BLA can improve recognition memory performance in tasks with neutral stimuli [2]. In one study [3], rats were presented with novel objects, and bouts of exploration of some of the objects were immediately followed by brief electrical stimulation of the BLA. When rats were tested one day later, recollection of objects that had been previously presented with stimulation was enhanced compared to that of objects that had not been paired with stimulation. Subsequent studies in rats found that electrical and optogenetic stimulation of the BLA elicited slow gamma (30–55 Hz) oscillations in the hippocampus and that inactivation of the hippocampus eliminated the memory enhancement resulting from BLA stimulation [3–5].

A recent study of patients with depth electrodes implanted in the medial temporal lobe (MTL) to monitor epileptic activity extended the rodent findings in three key respects [6]. First, the study found that direct electrical stimulation of the BLA in humans following the presentation of a neutral object led to better memory for the objects when memory was tested the subsequent day. Second, MTL LFP activity that occurred one day after encoding, during accurate recognition, differed between objects that had been previously presented with BLA stimulation versus those that had not. Third, stimulation was performed at low amplitudes which did not cause detectable changes in peripheral autonomic measures, and during formal testing, patients reported no awareness of the BLA stimulation, indicating that the memory enhancement did not appear to depend upon emotional arousal. Thus, data from rats and humans have indicated that direct stimulation of the BLA can enhance memory by modulating processes in the hippocampus and can do so without triggering overt emotional arousal.

Key unanswered questions, particularly for humans, involve the precise nature of amygdala-hippocampal network states favorable to memory and how direct electrical BLA stimulation may control such states. Quantifying the neurophysiological effects of brain stimulation and their link to subsequent behavior is crucial for understanding how specific activity patterns relate to cognitive processes. Interpretable machine learning classification models combined with feature learning techniques are effective tools for identifying neurophysiological features that predict memory performance [7]. Moreover, these techniques can be used to quantify the neurophysiological effects of stimulation by classifying between stimulated and unstimulated states based on the neural features.

While statistical inference techniques can be used to capture the relationship between neural features and cognitive states, they cannot be used for making predictions to inform closed-loop experiments or to optimize neuromodulation [3,8–10]. Besides, statistical inference may become less precise as the number of input variables increases. On the other hand, machine learning classification methods are focused on identifying generalizable patterns in high dimensional data for out-of-sample predictions [11]. Interpretable machine learning techniques have built-in measures that allow quantifying the contribution of each input variable to classification [12]. In the current study, we leveraged an interpretable machine learning approach to investigate the neurophysiological effects of amygdala stimulation and their relationship with biomarkers of successful memory processing in the amygdalo-hippocampal network.

2. Material and methods

2.1. Participants

Fourteen English-speaking adults (>18 years and five females) with drug-resistant epilepsy and implanted with intracranial depth electrodes in the BLA and hippocampus provided written informed consent to undergo amygdala stimulation and an image memory task [6]. The demographic information and memory performance results of each subject are provided in Table S1. The Emory University Institutional Review Board approved this research study.

2.2. Experimental procedure

During the study phase, 160 neutral object images were presented to the patients for 3 s. Unbeknownst to each participant, a random half of the images were followed by direct amygdala stimulation (labeled as “stimulation” trials), and the other half were considered as “no stimulation” trials (Fig. 1A and Fig. 1B). The amygdala was stimulated with 1 s of low-amplitude, rectangular pulses at 0.5 in 8 trains of 4 pulses at 50 Hz (theta-modulated gamma stimulation). These stimulation parameters were selected to mimic amygdalo-hippocampal theta-gamma activity patterns observed during successful encoding of items and item-context associations in prior experimental studies in animals and humans [3,13–16]. Such BLA stimulation parameters were subsequently demonstrated to enhance event-specific memory in several animal experiments [15–18] and in humans [6].

Fig. 1C shows three representative examples of the LFP signals recorded from a hippocampus depth electrode contact pair spanning the CA1 field during the study phase. The LFP signals from the hippocampus and amygdala were recorded during the entire study phase. The subjects' memory was tested via a self-paced yes/no (i.e., repeated/new) recognition-memory task for half the images (40 from the stimulated and 40 from the unstimulated trials) immediately after the end of the study session (i.e., “immediate” test); memory for the remaining images (40 from the stimulated and 40 from the unstimulated trials) was tested approximately one day later (i.e., “one-day” test; M_{delay} = 22 h, range = 20–25 h delay). Forty new images served as foils, and different foils were used for each test [6]. In our study, we used a discriminability index (d' index, a standard metric of recognition memory), to measure the participant's memory in an old/new recognition memory test (see Supplementary material for more details on the use of d' recognition memory scores) [19].

2.3. Localization of the stimulation and recording electrodes

The stimulation and recording contacts in each patient were determined by automated coregistration of each postoperative structural brain MRI and head computed tomography images with each preoperative brain MRI using a stereotactic neurosurgical planning computer workstation (ROSA Surgical Planning Software; MedTech Surgical, Inc.). Next, a neurosurgeon (JTW) compared the contact locations with standard MRI and tissue-section atlases of the human brain for precise localization of each electrode relative to each patient's medial temporal lobe anatomy [6].

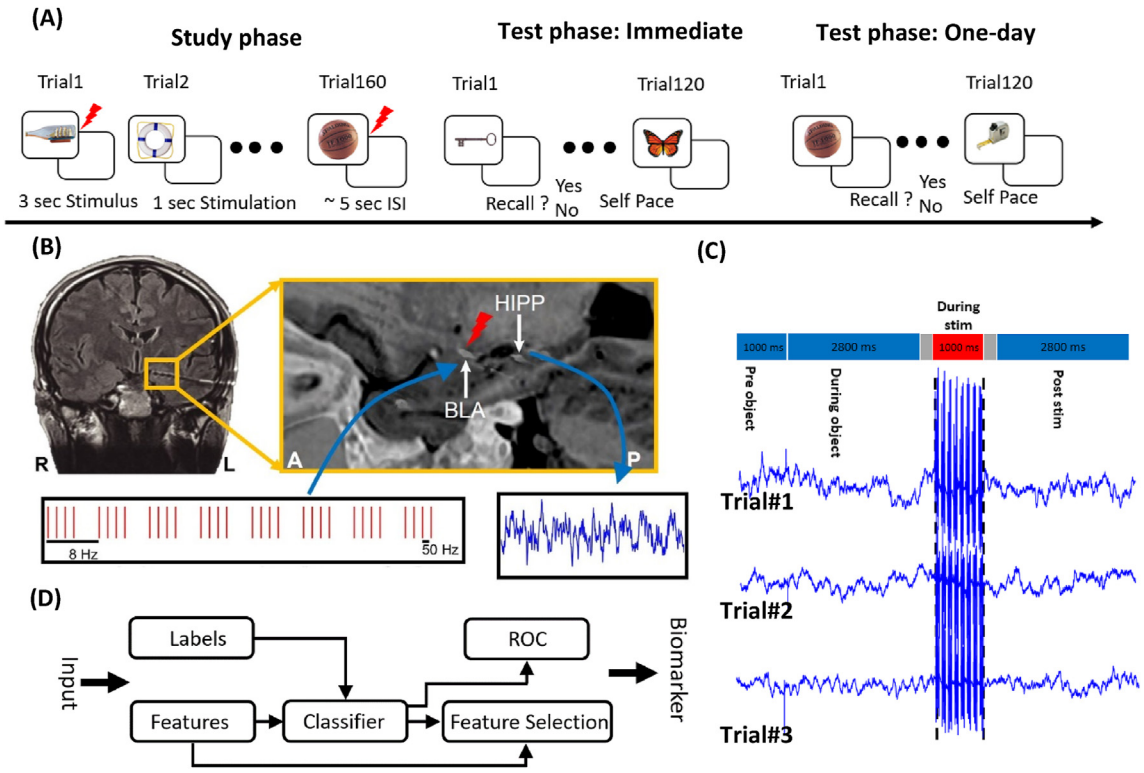

Fig. 1. Experimental and Analysis Procedure (A) Schematic of recognition memory task in which amygdala was stimulated following half of the objects in the study phase and recognition memory was tested on unique subsets of images immediately and one day after the study phase. **(B)** Representative, postoperative coronal MRI showing electrode contacts in the amygdala (white square). The red arrow shows the place of stimulation. **(C)** Representative signals recorded from hippocampus electrode contact pair nearest to CA1 for three trials 200 ms of the signals before and after stimulation (gray boxes) are not being used. **(D)** Spectral power (features) of the electrodes in the hippocampus and amygdala was used as input to fit a classifier to discriminate between two input groups based on their labels. Feature selection used the model generated by the classifier and the input features to find the biomarker that was most predictive in discriminating between the two states. . (For interpretation of the references to color in this figure legend, the reader is referred to the Web version of this article.)

2.4. Brain stimulation and recording

LFPs were recorded using depth electrodes (Ad-Tech; 0.86 mm diameter, 2 mm length platinum-coated contacts, typically spaced along with 5-mm intervals) and an amplifier (XLTEK EMU 128FS; Natus Medical) for each patient, at a sampling rate of either 500 or 1,000Hz. A research neurostimulator (CereStim M96; Blackrock Microsystems) was used to deliver the current regulated, charge-balanced, biphasic rectangular pulses at 0.5 mA for 1s in eight trains of four pulses at 50 Hz (theta-modulated gamma burst, Fig. 1B) to the BLA precisely at the offset of image presentation for a randomized half of the studied images. No seizure activity or after-discharges following stimulation were detected during testing or in a thorough post-test review of all recorded LFP channels by a clinical epileptologist.

2.5. Preprocessing

The LFP signals were first digitally filtered with a high pass cutoff of 1 Hz to attenuate low-frequency artifacts and a low pass cutoff of 249 Hz. The median LFP across all available recording electrodes was then subtracted from each LFP to remove non-local (global) artifacts. The signal was decomposed into the frequency components using Fast Fourier Transform, and power was averaged in standard bands, including θ (5–8 Hz), α (9–12 Hz), β (13–30 Hz), slow-γ (31–55 Hz), and fast-γ (65–90 Hz) [20]. We used the spectral power extracted from hippocampus and amygdala recordings as potential biomarkers.

2.6. Binary classification and feature learning

A logistic regression (LR) model was used to classify the neural states with spectral features of the LFPs as the input signal. The neural states (i.e., "good" memory vs. "bad" memory or Stim vs. No Stim) were labeled for the classification task. One of the main advantages of LR is the interpretability of the model. We leveraged this property to identify the important neural features that contributed to classification. To this end, we utilized the elastic net regularization (ENR) technique. Elastic net is a regularization and feature selection technique that simultaneously estimates the model parameters and selects the most important features by minimizing the cost function in (Eq. (1)&2).

$$\min_{\beta_0,\beta}\left(\frac{1}{2N}\sum_{i=1}^{N}\left(y_i-\beta_0-x_i^T\beta\right)^2+\lambda P_a(\beta)\right) \quad (1)$$

$$P_a(\beta)=\frac{(1-\alpha)}{2}\beta_2^2+\alpha|\beta|_1 \quad (2)$$

where N is the number of samples, y_i is the label of sample i, x_i is the feature of sample i, β and β_0 are the fitted coefficients, λ is the regularization parameters, and $P_a(\beta)$ is the penalty term in which a scalar coefficient (α) controls the contribution of *L1* and *L2* norms.

The idea is to achieve the best classification accuracy with as few model parameters as possible. This was accomplished by controlling the λ parameter in Eq. (1). As the λ increased (λ=0 in a non-regularized model), the model parameters were driven to 0. The

trajectory of the model parameters as a function of the regularization parameter (λ) formed the regularization path of the model. The features corresponding to the slowest decaying coefficients were interpreted as the most important ones [21,22].

The classification model parameters were estimated using N-folds nested cross-validation [23], where in each iteration, data were divided into training and test sets in the outer-fold. In the inner folds, the training data was further divided into training and validation sets. The best set of parameters were estimated by training different models using the inner-fold training data and validating using the validation data set. By sweeping the regularization parameter λ logarithmically from 10^{-5} to 10^{5} and the mixing parameter α between 0.8 and 0.95 in each inner-fold, we identified the optimal values of the hyperparameters that minimized the cross-validation error. We chose the range of α parameter close to 1 to prioritize model sparsification. The area under the curve (AUC) of receiver operating characteristic was calculated as a measure of the classifier's performance. To find the most informative feature in the model, we calculated the proportion of the models for which a given parameter was retained during the sweep of parameters in the inner fold. This measurement reflected the importance of a feature in the classification between two groups. The importance of a specific feature is relative to the other input features in the classification between two classes. The statistical significance of the relative importance of the features was calculated using a one-way analysis of variance (ANOVA) (Fig. 1D). This study utilized a repeated measures ANOVA (rmANOVA) test for statistical comparisons between "remembered" and "not-remembered" and between stimulated and unstimulated LFP features. All p-values have been adjusted for multiple comparisons using the Benjamini-Hochberg correction method [24]. We used Pearson linear correlation coefficients for the correlation analysis.

3. Results

3.1. Theta and gamma power in the hippocampus predict subsequent memory performance

The first step towards identifying the neurophysiological effects of memory-enhancing BLA stimulation was to investigate the neural processes underlying "good" memory performance in the absence of stimulation. To this end, we labeled the successfully and unsuccessfully "remembered" trials in the image recognition task as "good" and "bad" memory trials, respectively. 2800 ms of the LFP recordings from hippocampal electrodes nearest CA1 (hippocampus-CA1) and from the amygdala during the presentation of each image (named "during object", hereafter, Fig. 1C) were used to determine "good" and "bad" memory states when paired with the subsequent memory result. This time-window length was chosen to accurately estimate the lower end of the theta frequency band [25]. We focused on hippocampal CA1 due to the critical role in memory formation in humans and it's strong and direct connectivity to the BLA [26,27]. Moreover, it was the only hippocampal subregion that was sampled consistently in almost all (12 out of 14) subjects. This initial analysis focused on "no stimulation" trials to explore biomarkers in the absence of any potential confounding effect of stimulation. The spectral power from hippocampus-CA1 and the amygdala during each trial of the study phase in each of the twelve subjects formed the input vectors for the classification. The labels extracted from the subsequent recognition memory test were used to train a LR model with ENR. Since, we had imbalance labeled (imbalance number of "remembered" and "not remembered" trials) for each individual, we combined data from all subjects. To account for the subject variability, we used a leave-one subject-out approach in which one subject was used for testing, and the remaining eleven subjects were used for training. The trained model was used to predict memory performance in the test phase based on the LFP spectral powers of hippocampus-CA1 and amygdala during the study phase.

Fig. 2A shows the receiver operating characteristic (ROC) curve of classification between the "remembered" and "not-remembered" memory trials for the "immediate" test based on the hippocampus-CA1 LFP spectral features during the study phase. We used a leave-one subject-out (12-fold) nested cross-validation (mean AUC: 0.7182 ± 0.0828, $n = 12$, comparison with chance level $p < 0.001$, see Supplementary material) to evaluate the classifier's out-of-sample performance. Fig. 2B shows that theta power during the encoding phase was significantly more important than the other features in predicting "good" vs "bad" memory performance. ($p_{corrected}<0.01$). Fig. 2C, in which performance for each individual is calculated by subtracting remembered from non-remembered for each subject, shows that successfully remembering a picture in the "immediate" test is associated with higher theta power of the hippocampus-CA1 during the prior study phase (rmANOVA, $F(1,11) = 5.6$, $p_{corrected} = 0.04$). More specifically, we averaged the power of all "remembered" trials and "non-remembered" trials for each of 12 subjects in any specific band. Therefore, we had 12 values for the "remembered" and 12 values for the "not-remembered" trials. We used rmANOVA to statistically compare the 12 values of the remembered trials with non-remembered trials.

We used the same leave-one subject-out (12-fold) nested cross-validation approach to train and evaluate the LR model with ENR to predict the "remembered" and "not-remembered" trials in the "one-day" test based on the spectral features of the LFP recordings during the study phase. The ROC curve of this classification is based on the hippocampus-CA1 LFP features as the input is shown in Fig. 2D (mean AUC: 0.6561 ± 0.0842, $n = 12$, comparison with chance level $p < 0.001$). Fig. 2E shows that hippocampus-CA1 slow-gamma was the most important feature that predicted differences between the "not-remembered" and "remembered" trials during the "one-day" test ($p_{corrected}<0.01$). In addition, Fig. 2F shows that hippocampus-CA1 slow-gamma power was significantly higher in "remembered" compared to "not-remembered" trials ($F(1,10) = 4.63$ uncorrected $p = 0.04$). Using the interquartile range rule [28], one outlier was detected and removed from the statistical analysis.

3.2. Amygdala stimulation modulates hippocampal gamma activity

Understanding how amygdala stimulation impacts biomarkers associated with memory performance could help guide the design of closed-loop neuromodulation therapies for improving memory. To begin addressing this question, we explored the neurophysiological effects of BLA stimulation on hippocampus activity recorded from electrodes nearest CA1. 2800-ms continuous segments of the hippocampus-CA1 LFP recordings after each stimulation were extracted. To minimize any residual artifacts of the stimulation, 200 ms after the stimulation offset was excluded, as shown in Fig. 1C [29] (see Supplementary Fig. S1). The spectral power of the hippocampus-CA1 LFPs in different electrophysiological frequency bands was used as the input feature vector to train an LR classifier using ENR to classify between "stimulation" and "no stimulation" trials (Fig. 3A). Notably, we had equal numbers of stimulation and no stimulation trials gathered from each subject. As such, within each subject, we trained a model using a 10-fold nested cross-validation method in which 90% of the data was used for training and evaluating (in inner folds) the model, and the other 10% was used to test the out-of-sample generalization performance of the model. The ROC curve in Fig. 3B shows the performance of the classifier in discriminating between the stimulated and the

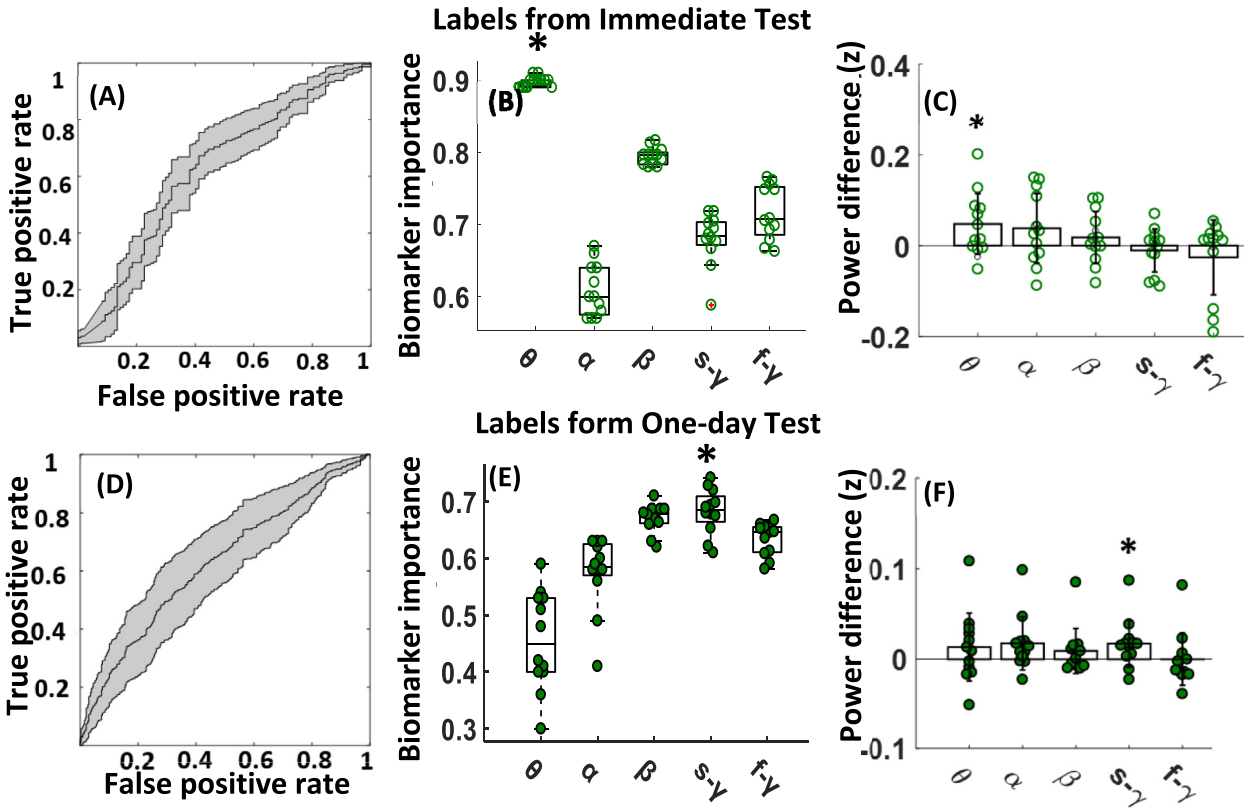

Fig. 2. Predicting memory performance in the "immediate" test and "one-day" test phase based on the CA1 activities during the study phase: (A) ROC for LR with ENR prediction of "remembered" versus "not-remembered" trials using CA1 signal in the "immediate test" (mean AUC: 0.7182 ± 0.0828, n = 12, comparison with chance level $p < 0.001$). **(B)** Biomarker importance graph for classification between "remembered" and "not-remembered" trials using CA1 signal and combining all subjects with 12-fold nested cross-validation. This graph shows that the theta band contributes most in classification between these two groups (corrected $p < 0.01$). In this figure, each dot represents the model that was used for any individual to predict their subsequent memory performance. Each red cross (+) represents an outlier in the boxplot.**(C)** Power difference between "remembered" and "not-remembered" trials using CA1 signal. The "remembered" trials show more power in theta band (rmANOVA $F(1,11) = 5.6$ corrected $p = 0.04$). In this graph each point represents the power difference between different trial types ("remembered" vs "not-remembered") for each individual. No significant outlier has been detected in theta band. **(D)** ROC of LR with ENR prediction of "remembered" versus "not-remembered" trials using CA1 signal (mean AUC: 0.6561 ± 0.0842, n = 12, comparison with chance level $p < 0.001$). **(E)** CA1 biomarker importance graph for classification between "remembered" and "not-remembered" trials combining all subjects with 12-fold nested cross-validation (corrected $p < 0.01$). This graph shows that the slow-gamma power in the CA1 contributed most in classification between these two groups. Each dot represents one subject. **(F)** Power difference between "remembered" and "not-remembered" trials in CA1 signal. The "remembered" trials show more power in CA1 slow-gamma band (rmANOVA $F(1,10) = 4.63$ uncorrected $p = 0.04$).). Each point represents one subject. We have removed the outlier in the statistical test. Each point represents one subject. (For interpretation of the references to color in this figure legend, the reader is referred to the Web version of this article.)

unstimulated trials for the 12 subjects, using hippocampus-CA1 LFP features after the stimulation offset. The AUC of the classifier with 10-fold nested cross-validation across all subjects was 0.70 ± 0.07 (comparison with chance level $p < 0.001$), which indicates significant changes in the hippocampus-CA1 LFP features post-stimulation. Fig. 3C shows a representative importance graph, which reflects the contribution of each frequency band in classifying between stimulated and unstimulated trials for one subject. As this figure shows, slow gamma activity has the most contribution in this classification ($p_{corrected}<0.01$, n = 1). Also, Fig. 3D shows the power difference (stimulated vs. unstimulated trials) in distinct frequency bands. A significant increase in the slow-gamma band was observed (unstimulated: mean = 0.3422, sd = 0.02, stimulated: mean = 0.3803, sd = 0.0192, $p_{corrected}$ <0.01). The feature selection results for each subject are shown in Fig. S3.

3.3. Amygdala stimulation may heterogeneously modulate subregions of the hippocampal formation

Spectral power features, using the same 2800-ms post-stimulation window, were extracted from the bipolar LFP recordings from electrode pairs localized in the subiculum (SUB, number of subject or N = 10), CA1, dentate gyrus (DG, N = 5), and the parahippocampal cortex (PHC, N = 9). LR classification models with ENR were trained using 10-fold nested cross-validation to discriminate between stimulated and unstimulated trials in each region. Fig. 4A shows the mean and standard deviation of the classifier performance in different regions across subjects. A higher classification accuracy indicates greater separability in the feature space and suggests a stronger neuromodulatory effect of amygdala stimulation. As this figure demonstrates, memory-enhancing amygdala stimulation had a stronger neuromodulatory effect upon LFPs recorded nearest the SUB compared to other subregions of the hippocampal formation (mean AUC: 0.7286 ± 0.0752, n = 10). However, no significant difference was observed on the AUC of different hippocampal subregions. An additional correlation analysis did not show an association between the distance between the stimulation site and the recording electrode (from CA1) and change in slow-gamma power as an effect of stimulation (See Supplementary Material Fig. S4). Fig. 4B compares the theta power between stimulated and unstimulated trials in possibly different regions of the hippocampal formation. The rmANOVA test showed

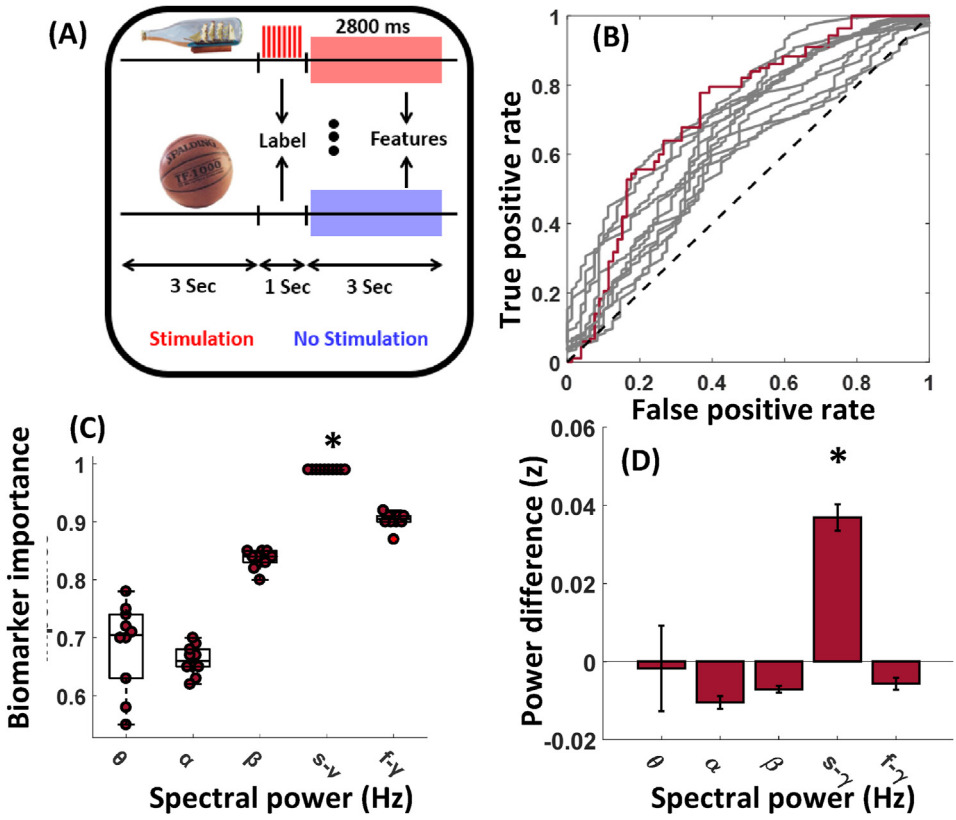

Fig. 3. The neuromodulatory effect of amygdala stimulation on the hippocampal activities: (A) Post-stimulation of the (CA1) LFPs of "stimulation" and "no stimulation" were segmented to create features. **(B)** Individual classification ROC curves for each individual subject (mean AUC = 0.70 ± 0.07, n = 12). In this graph, each line represents one subject. The color line is the representative subject **(C)** A representative biomarker importance graph for classifying between the post-stimulation state of stimulated and unstimulated trials (corrected $p < 0.01$, n = 1). The represented subject ROC has been marked by different color in Panel B. **(D)** Stimulated and unstimulated power in different electrophysiological bands. The power in the low-gamma band is greater in the stimulated trial (unstimulated: mean = 0.3422, sd = 0.02, stimulated: mean = 0.3803, sd = 0.0192, corrected $p < 0.01$). (For interpretation of the references to color in this figure legend, the reader is referred to the Web version of this article.)

a significant difference in theta power between stimulated and unstimulated trials in LFPs nearest PHC ($p_{corrected} = 0.04$, n = 9), and no significant difference in theta power was observed in the other regions. Fig. 4C shows the results of the same analysis for slow-gamma power. Again, amygdala stimulation was associated with a significant increase in gamma activity in LFPs nearest the SUB ($p_{corrected} = 0.01$, n = 10) and the CA1 ($p_{corrected} = 0.04$, n = 12) regions. However, the BLA stimulation did not significantly affect the slow-gamma power of the LFPs recorded nearest the other regions.

Given the potential for modulatory effects of amygdala stimulation upon CA1, SUB, and PHG subregions, we examined this effect's relationship to subsequent memory performance (supplementary material and Fig. S5). Specifically, we examined potential correlations between theta power in PHG and slow-gamma in CA1 and SUB with memory performance at "immediate" and One-day test time points. Notably, only the positive correlation of slow-gamma in CA1 to memory performance at the One-day test was observed to be statistically significant.

4. Discussion

Neural activity, measured by LFPs during emotional and memory tasks, can be used as biomarkers to understand the effects of direct brain stimulation on memory processing network dynamics [8,30]. In this study, we used LR classification with ENR to differentiate between "remembered" and "not-remembered" trials in the "immediate" and "one-day" tests, based on LFP features recorded nearest CA1 (Fig. 2) and the amygdala (See Fig. S2). The ENR was used as a feature learning method to identify the most important features that discriminated between "remembered" and "not-remembered" trials. We found an increase in the hippocampal CA1 theta power during the encoding phase was the most important feature that discriminated between "remembered" and "not-remembered" trials of the "immediate" test. Indeed, the hippocampal theta rhythm is a prominent biomarker of spatial memory, and memory in general, in human and animal models [31–33]. Several human studies have demonstrated that hippocampal theta activation during encoding predicted subsequent memory performance [34–36]. In particular, theta rhythm was a predictor of the memory performance in the short-term memory test [37,38]. Moreover, theta power before the presentation of stimuli predicts the subsequent remembering performance of successful episodic memory retrieval [39]. Likewise, Backus et al. [35] showed an increase in hippocampal theta activity while a new memory is successfully combined with an existing mnemonic representation, and Lin et al. [17], which showed that theta power increases during successful item encoding.

We found that the spectral band features that differentiated between "remembered" and "not-remembered" trials in the "one-day" test included slow-gamma power recorded within the sampled locations in the medial temporal lobe from hippocampus-CA1 and theta power recorded from the amygdala. Although we could not histologically verify that human recordings represent signals specific to these locations, the results are generally in agreement with the results of other animal and human studies.

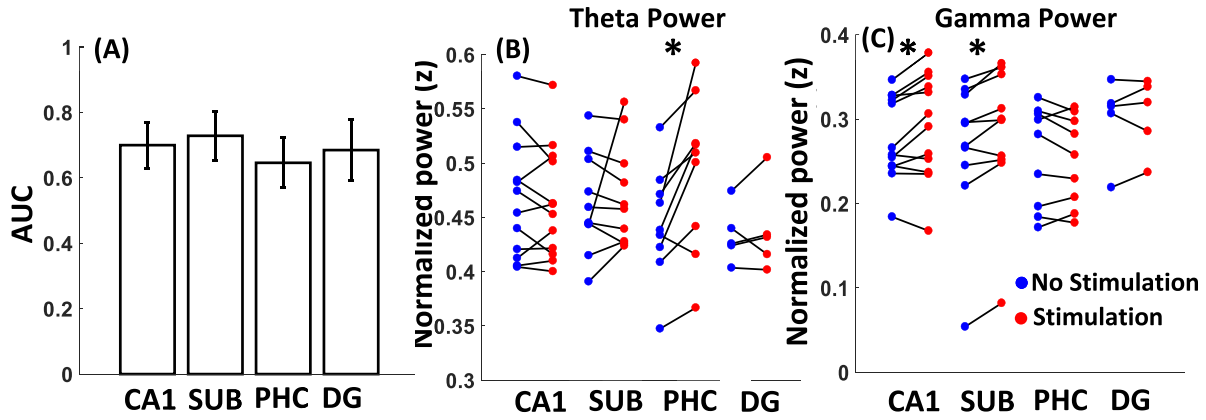

Fig. 4. Neuromodulatory effect of direct amygdala stimulation on different hippocampal sub-regions. (A) AUC values for classification between stimulated and unstimulated trials based on the spectral features of post-stimulation LFP recordings in CA1, Subiculum (SUB), Dentate Gyrus (DG), and Para-Hippocampal Cortex (PHC). Stimulation has more neuromoulatory effect on SUB (mean AUC: 0.7286 ± 0.0752, n = 10). **(B)** Normalized power of theta band in CA1, SUB, DG, and PHC for stimulated (red) and unstimulated (blue) trials. RmANOVA shows a significant difference in PHC (corrected p = 0.04, n = 9), which means amygdala stimulation significantly increases theta power in PHC. **(C)** Normalized power of gamma band in CA1, SUB, DG, and PHC for stimulated (red) and unstimulated (blue) trials. RmANOVA shows a significant change in CA1 (corrected p = 0.04, n = 12) and SUB (corrected p = 0.01, n = 10) slow-gamma power. Amygdala stimulation significantly increases slow-gamma power in CA1 and SUB. In this graph, the red dots show the stimulated ("stimulation") and blue dots show the unstimulated ("no stimulation") trials. (For interpretation of the references to color in this figure legend, the reader is referred to the Web version of this article.)

Trimper et al. [40] showed an increase in the slow-gamma power in the physiologically- and histologically-defined CA1 when rats explored an object during encoding. Also, Jutras et al. [41] show that greater hippocampal gamma power during encoding predicted greater subsequent visual recognition memory performance in macaque monkeys. Human studies likewise showed that broadband gamma power in the hippocampus and the left temporal and frontal-parietal cortices is a neurophysiological predictor of successful encoding during the memory tasks [42,43].

We used our classification approach to identify spectral features of hippocampal LFPs that were modulated by amygdala stimulation. Our results demonstrated that slow-gamma power was the most important neurophysiological feature that discriminated between stimulated and unstimulated trials and that amygdala stimulation particularly increased slow-gamma power in the hippocampus near CA1. Similarly, optogenetic stimulation of the rat amygdala with analogous stimulation parameters increased gamma power in CA1 [44]. Taken together, the mechanisms that govern hippocampal gamma induction by amygdala stimulation are likely fundamentally similar in rats and humans. Recent studies have linked emotional memory to increases in gamma power in the amygdala as well [45–47]. We have previously demonstrated that electrically stimulating the amygdala directly without eliciting awareness, subjective emotions, or autonomic responses but still enhanced memory for non-emotional objects in the subjects used for this analysis [6]. Although the current study is not able to demonstrate that these changes in post-stimulation slow-gamma power are directly related memory enhancement, the increases in slow-gamma power for remembered relative to forgotten items suggest an enticing link between these hippocampal signal changes. Future studies that address the limitations of our study are directly designed to address whether stimulation directly modulates successful memory biomarkers will be needed.

Although we did not observe a significant difference in AUC of stimulation vs. no stimulation classification across all subregions of the hippocampus, we found that amygdala stimulation differentially affects the hippocampal subregions. Amygdala stimulation increases the slow-gamma power in CA1 and SUB and the theta power in PHG (Fig. 4B and C). While we found that the amygdala stimulation significantly increased slow gamma power nearest the CA1 and SUB and increased theta nearest PHG, our findings do not exclude the possibility that additional neurophysiological features or anatomic structures may be relevant but detectable with additional methods or only in larger samples with denser electrode sampling of hippocampal subfields.

5. Conclusion

We presented a machine learning approach that utilized classification-based feature learning for investigating the neurophysiological effects of memory-enhancing amygdala stimulation and their link to memory processes. Neurophysiological states of the amygdala and hippocampus during the encoding phase and before stimulation delivery predict subsequent memory. In particular, gamma power in CA1 may be correlated with subsequent memory performance. Finally, we found that amygdala stimulation immediately increases CA1 gamma activity, and this change correlates with behavioral outcomes in a memory recognition test. The effect of amygdala stimulation upon CA1 gamma power may elucidate a potential mechanism by which amygdala stimulation enhances memory over time, however future studies will be necessary to directly link these two findings.

CRediT authorship contribution statement

Mohammad S.E. Sendi: Methodology, Formal analysis, Software, Visualization, Writing – original draft, Writing – review & editing. **Cory S. Inman:** Conceptualization, Methodology, Investigation, Data curation, Supervision, Project administration, Writing – review & editing. **Kelly R. Bijanki:** Investigation, Data curation, Methodology. **Lou Blanpain:** Formal analysis, Data curation, Methodology, Visualization. **James K. Park:** Data curation, Methodology. **Stephan Hamann:** Conceptualization, Methodology. **Robert E. Gross:** Supervision, Resources. **Jon T. Willie:** Conceptualization, Methodology, Investigation, Supervision, Resources, Project administration, Writing – review & editing, Funding acquisition. **Babak Mahmoudi:** Conceptualization, Methodology, Supervision, Project administration, Writing – review & editing, Funding acquisition.

Declaration of competing interest

No conflicts of interest apply.

7. Acknowledgments

We thank the patients that participated in our research for their time and trust in completing our research. We would also like to thank the epilepsy techs, physicians, nurses, and staff at Emory University for their support with our research. Finally, we appreciate Emily Chen's time and effort localizing electrodes across all of our participants. Funding support was provided by the National Institutes of Health UG3NS100559 and 1R01EB028350.

Appendix A. Supplementary data

Supplementary data to this article can be found online at https://doi.org/10.1016/j.brs.2021.09.009.

8. Data availability

The datasets generated for this study are available on request to the corresponding author.

References

[1] LaBar KS, Cabeza R. Cognitive neuroscience of emotional memory. Nat Rev Neurosci 2006;7:54–64. https://doi.org/10.1038/nrn1825.
[2] McGaugh JL. The amygdala modulates the consolidation of memories of emotionally arousing experiences. Annu Rev Neurosci 2004;27:1–28. https://doi.org/10.1146/annurev.neuro.27.070203.144157.
[3] Bass David I Jrm. Memory-enhancing amygdala stimulation elicits gamma synchrony in the hippocampu. Behav Neurosci 2015;129:244–56. https://doi.org/10.1037/bne0000052.Memory-Enhancing.
[4] Sharp BM. Basolateral amygdala and stress-induced hyperexcitability affect motivated behaviors and addiction. Transl Psychiatry 2017;7:e1194. https://doi.org/10.1038/tp.2017.161.
[5] Bass DI, Nizam ZG, Partain KN, Wang A, Manns JR. Amygdala-mediated enhancement of memory for specific events depends on the hippocampus. Neurobiol Learn Mem 2014;107:37–41. https://doi.org/10.1016/j.nlm.2013.10.020.
[6] Inman CS, Manns JR, Bijanki KR, Bass DI, Hamann S, Drane DL, et al. Direct electrical stimulation of the amygdala enhances declarative memory in humans. Proc Natl Acad Sci Unit States Am 2018;115:98–103. https://doi.org/10.1073/pnas.1714058114.
[7] Cai J, Luo J, Wang S, Yang S. Feature selection in machine learning: a new perspective. Neurocomputing 2018;300:70–9. https://doi.org/10.1016/j.neucom.2017.11.077.
[8] Butler JL, Paulsen O. Hippocampal network oscillations - recent insights from in vitro experiments. Curr Opin Neurobiol 2015;31:40–4. https://doi.org/10.1016/j.conb.2014.07.025.
[9] Mohan UR, Watrous AJ, Miller JF, Lega BC, Sperling MR, Worrell GA, et al. The effects of direct brain stimulation in humans depend on frequency, amplitude, and white-matter proximity. Brain Stimulation 2020;13:1183–95. https://doi.org/10.1016/j.brs.2020.05.009.
[10] Bronte-Stewart H, Barberini C, Koop MM, Hill BC, Henderson JM, Wingeier B. The STN beta-band profile in Parkinson's disease is stationary and shows prolonged attenuation after deep brain stimulation. Exp Neurol 2009;215:20–8. https://doi.org/10.1016/j.expneurol.2008.09.008.
[11] Habets JGV, Janssen MLF, Duits AA, Sijben LCJ, Mulders AEP, Greef B De, et al. Machine learning prediction of motor response after deep brain stimulation in Parkinson's disease—proof of principle in a retrospective cohort. PeerJ 2020;8:1–17. e10317.
[12] Bzdok D, Altman N, Krzywinski M. Points of significance: statistics versus machine learning. Nat Methods 2018;15:233–4. https://doi.org/10.1038/nmeth.4642.
[13] Fell J, Klaver P, Lehnertz K, Grunwald T, Schaller C, Elger CE, et al. Human memory formation is accompanied by rhinal-hippocampal coupling and decoupling. Nat Neurosci 2001;4:1259–64. https://doi.org/10.1038/nn759.
[14] Tort ABL, Komorowski RW, Manns JR, Kopell NJ, Eichenbaum H. Theta-gamma coupling increases during the learning of item-context associations. Proc. Natl. Acad. Sci. U.S.A 2009;106. https://doi.org/10.1073/pnas.0911331106. 20942–7.
[15] Bass DI, Nizam ZG, Partain KN, Wang A, Manns JR. Amygdala-mediated enhancement of memory for specific events depends on the hippocampus. Neurobiol Learn Mem 2014;107:37–41. https://doi.org/10.1016/j.nlm.2013.10.020.
[16] Bass DI, Partain KN, Manns JR. Event-specific enhancement of memory via brief electrical stimulation to the basolateral complex of the amygdala in rats. Behav Neurosci 2012;126:204–8. https://doi.org/10.1037/a0026462.
[17] Lin JJ, Rugg MD, Das S, Stein J, Rizzuto DS, Kahana MJ, et al. Theta band power increases in the posterior hippocampus predict successful episodic memory encoding in humans. Hippocampus 2017;27:1040–53. https://doi.org/10.1002/hipo.22751.
[18] Bass DI, Partain KN, Manns JR. Event-specific enhancement of memory via brief electrical stimulation to the basolateral complex of the amygdala in rats. Behav Neurosci 2013;126:204–8. https://doi.org/10.1037/a0026462.Event-Specific.
[19] Neath I, Surprenant AM. Human memory : an introduction to research, data, and theory. second ed. Belmont, CA: Wadsworth.; 2003.
[20] Stoica P, Moses R. Spectral analysis of signals. Upper Saddle River, NJ: Prentice Hall; 2005. https://doi.org/10.1109/msp.2007.273066.
[21] Zou H, Hastie T. Erratum: regularization and variable selection via the elastic net. J Roy Stat Soc B: Statistical Methodology (2005) 67 (301-320)). Journal of the Royal Statistical Society Series B: Statistical Methodology 2005;67:768. https://doi.org/10.1111/j.1467-9868.2005.00527.x.
[22] Tibshiran R. Regression shrinkage and selection via the lasso: a retrospective. JRStatistSoc 2011;73:273–82. https://doi.org/10.1111/j.1439-0264.1997.tb00113.x.
[23] Wainer J, Cawley G. Nested cross-validation when selecting classifiers is overzealous for most practical applications. ArXiv 2018:1–9.
[24] Benjamini Yoav, Yosef Hochberg. Controlling the false discovery Rate : a practical and powerful approach to multiple testing. Royal Statistical Society Series B (Methodological) 1995;57:289–300.
[25] Reinhart RMG, Nguyen JA. Working memory revived in older adults by synchronizing rhythmic brain circuits. Nat Neurosci 2019;22:820–7. https://doi.org/10.1038/s41593-019-0371-x.
[26] Bartsch T, Döhring J, Rohr A, Jansen O, Deuschl G. CA1 neurons in the human hippocampus are critical for autobiographical memory , mental time travel , and autonoetic consciousness. Proc Natl Acad Sci Unit States Am 2011;108:17562–7. https://doi.org/10.1073/pnas.1110266108.
[27] Wang XJ, Barbas XH. Specificity of primate amygdalar pathways to Hippocampus. J Neurosci 2018;38:10019–41.
[28] Kokoska S, Zwillinger D. CRC standard probability and statistics tables and formulae. Student Edition 2000. https://doi.org/10.1201/b16923.
[29] Solomon EA, Kragel JE, Gross R, Lega B, Sperling MR, Worrell G, et al. Medial temporal lobe functional connectivity predicts stimulation-induced theta power. Nat Commun 2018;9:1–13. https://doi.org/10.1038/s41467-018-06876-w.
[30] Headley DB, Paré D. Common oscillatory mechanisms across multiple memory systems. Npj Science of Learning 2017;2. https://doi.org/10.1038/s41539-016-0001-2. 0–1.
[31] Itskov V, Pastalkova E, Mizuseki K, Buzsaki G, Harris KD. Theta-mediated dynamics of spatial information in hippocampus. J Neurosci 2008;28:5959–64. https://doi.org/10.1523/JNEUROSCI.5262-07.2008.
[32] Buzsáki G, Moser EI. Memory, navigation and theta rhythm in the hippocampal-entorhinal system. Nat Neurosci 2013;16:130–8. https://doi.org/10.1038/nn.3304.
[33] Bezaire MJ, Raikov I, Burk K, Vyas D, Soltesz I. Interneuronal mechanisms of hippocampal theta oscillations in a full-scale model of the rodent CA1 circuit. ELife 2016;5. https://doi.org/10.7554/eLife.18566.
[34] Cohen MX. Hippocampal-prefrontal connectivity predicts midfrontal oscillations and long-term memory performance. Curr Biol 2011;21. https://doi.org/10.1016/j.cub.2011.09.036. 1900–5.
[35] Backus AR, Schoffelen JM, Szebényi S, Hanslmayr S, Doeller CF. Hippocampal-prefrontal theta oscillations support memory integration. Curr Biol 2016;26:450–7. https://doi.org/10.1016/j.cub.2015.12.048.
[36] Bohbot VD, Copara MS, Gotman J, Ekstrom AD. Low-frequency theta oscillations in the human hippocampus during real-world and virtual navigation. Nat Commun 2017;8:1–7. https://doi.org/10.1038/ncomms14415.
[37] Vertes RP. Hippocampal theta rhythm: a tag for short-term memory. Hippocampus 2005;15:923–35.
[38] Babiloni C, Vecchio F, Mirabella G, Buttiglione M, Sebastiano F, Picardi A, et al. Hippocampal , amygdala , and neocortical synchronization of theta rhythms is related to an immediate recall during rey auditory verbal learning test. Hum Brain Mapp 2009:2077–89. https://doi.org/10.1002/hbm.20648.
[39] Addante RJ, Watrous AJ, Yonelinas AP, Ekstrom AD, Ranganath C. Prestimulus theta activity predicts correct source memory retrieval. Proc. Natl. Acad. Sci. U.S.A 2011;108. https://doi.org/10.1073/pnas.1014528108. 10702–7.
[40] Trimper JB, Galloway CR, Jones AC, Mandi K, Manns JR. Gamma oscillations in rat hippocampal subregions dentate gyrus, CA3, CA1, and subiculum underlie associative memory encoding. Cell Rep 2017;21:2419–32. https://doi.org/10.1016/j.celrep.2017.10.123.
[41] Jutras MJ, Fries P, Buffalo EA. Gamma-band synchronization in the macaque Hippocampus and memory formation. J Neurosci 2009;29:12521–31. https://doi.org/10.1523/jneurosci.0640-09.2009.
[42] Ezzyat Y, Kragel JE, Burke JF, Levy DF, Lyalenko A, Wanda P, et al. Direct brain stimulation modulates encoding states and memory performance in humans. Curr Biol 2017;27:1251–8. https://doi.org/10.1016/j.cub.2017.03.028.
[43] Sederberg PB, Schulze-Bonhage A, Madsen JR, Bromfield EB, McCarthy DC, Brandt A, et al. Hippocampal and neocortical gamma oscillations predict

memory formation in humans. Cerebr Cortex 2007;17:1190–6. https://doi.org/10.1093/cercor/bhl030.
[44] Ahlgrim NS, Manns JR. Optogenetic stimulation of the basolateral amygdala increased theta-modulated gamma oscillations in the Hippocampus. Front Behav Neurosci 2019;13:1–13. https://doi.org/10.3389/fnbeh.2019.00087.
[45] Headley DB, Paré D. In sync: gamma oscillations and emotional memory. Front Behav Neurosci 2013;7:1–12. https://doi.org/10.3389/fnbeh.2013.00170.
[46] Sato W, Kochiyama T, Uono S, Matsuda K, Usui K, Inoue Y, et al. Rapid amygdala gamma oscillations in response to fearful facial expressions. Neuropsychologia 2011;49:612–7. https://doi.org/10.1016/j.neuropsychologia.2010.12.025.
[47] Luo Q, Holroyd T, Jones M, Hendler T, Blair J. Neural dynamics for facial threat processing as revealed by gamma band synchronization using MEG. Neuroimage 2007;34:839–47. https://doi.org/10.1016/j.neuroimage.2006.09.023.